Supporting Information

Synthesis and Quantum Metrology of Metal-Organic Framework-Coated Nanodiamonds Containing Nitrogen Vacancy Centers

Roman A. Shugayev,*[,†,§] Scott E. Crawford,*[,†,§] John P. Baltrus,[†] Nathan A. Diemler,[†,‡] James E. Ellis,[†] Ki-Joong Kim,[†,‡] and Patricia C. Cvetic[†,‡]

[†]National Energy Technology Laboratory, 626 Cochrans Mill Road, Pittsburgh, Pennsylvania 15236, United States

[‡]Leidos Research Support Team, 626 Cochrans Mill Road, Pittsburgh, Pennsylvania 15236, United States

[§]These authors contributed equally.

Table of Contents:

Figure S1. Photograph of NDs@ZIF-8 solution taken 1 hour after synthesis.

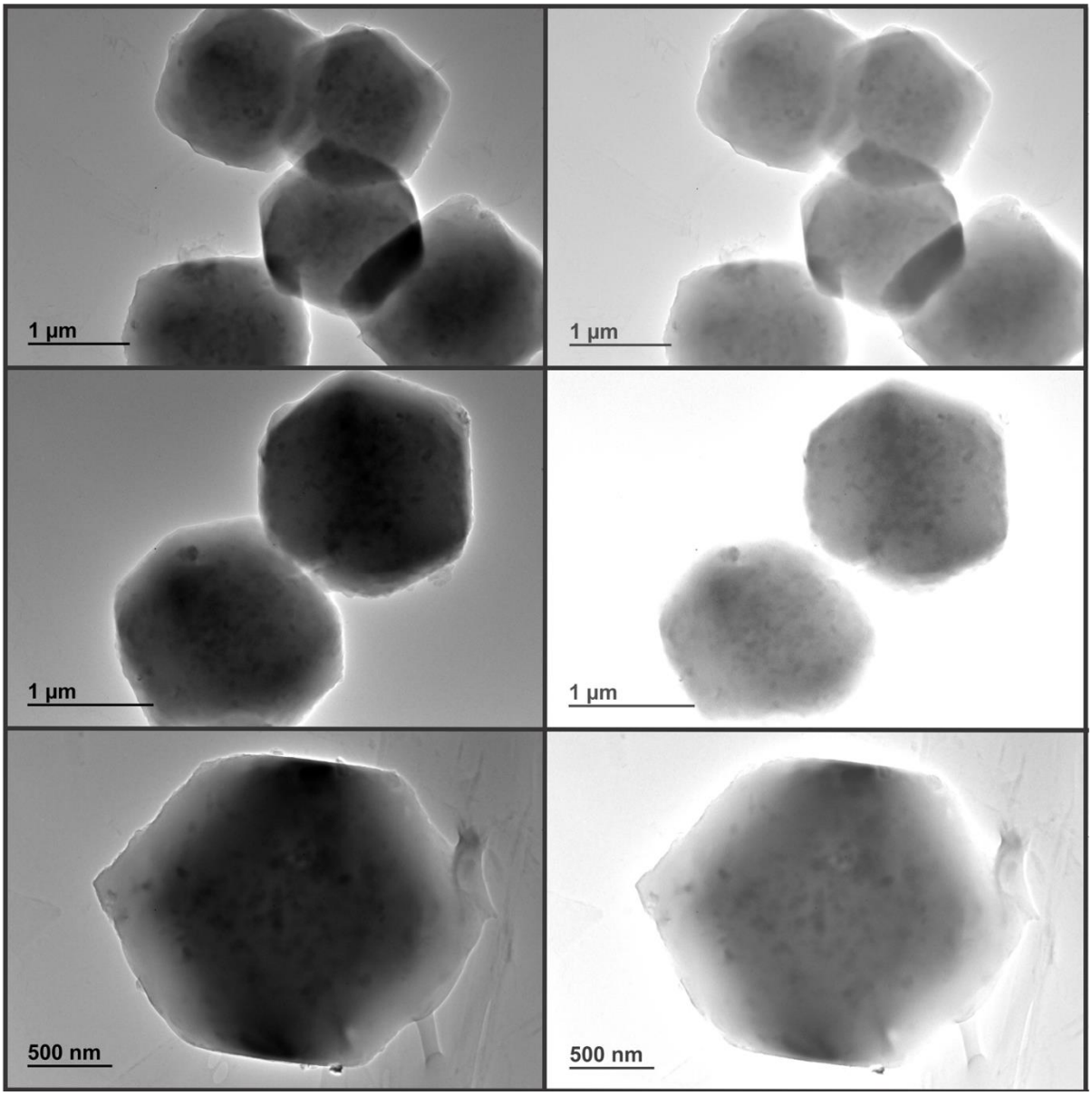

Figure S2. Wideout transmission electron microscopy image of different NDs@ZIF-8 composites. Small areas of darker contrast are consistent in size (~70 nm) and morphology of nanodiamonds. The left column shows the original TEM images, and right column shows the same images with the brightness and contrast adjusted using ImageJ to more clearly display the nanodiamonds.

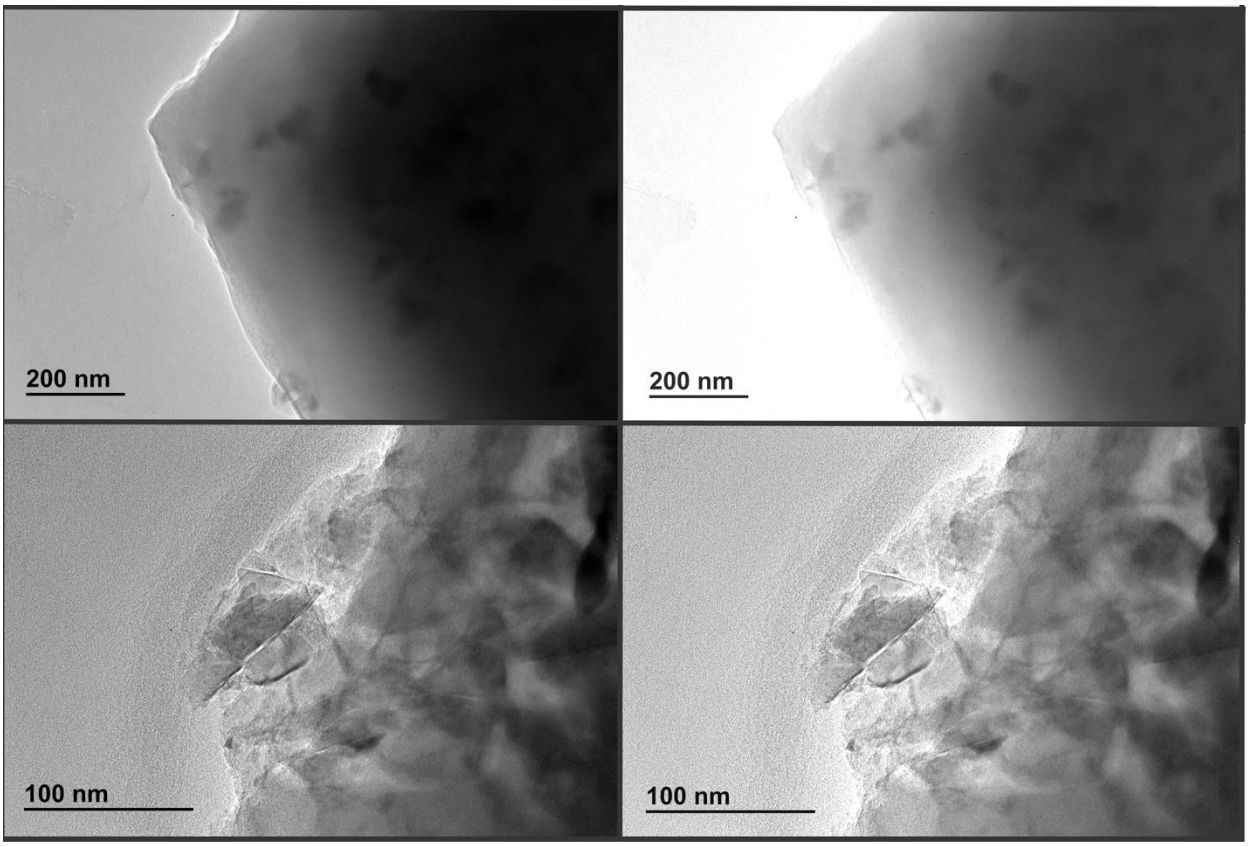

Figure S3. Transmission electron microscopy images of different NDs@ZIF-8 composites taken at a higher magnification than those in Figure S2. Small areas of dark contrast are consistent in size (~70 nm) and morphology of nanodiamonds. The left column shows the original TEM images, and right column shows the same images with the brightness and contrast adjusted using ImageJ to more clearly display the nanodiamonds.

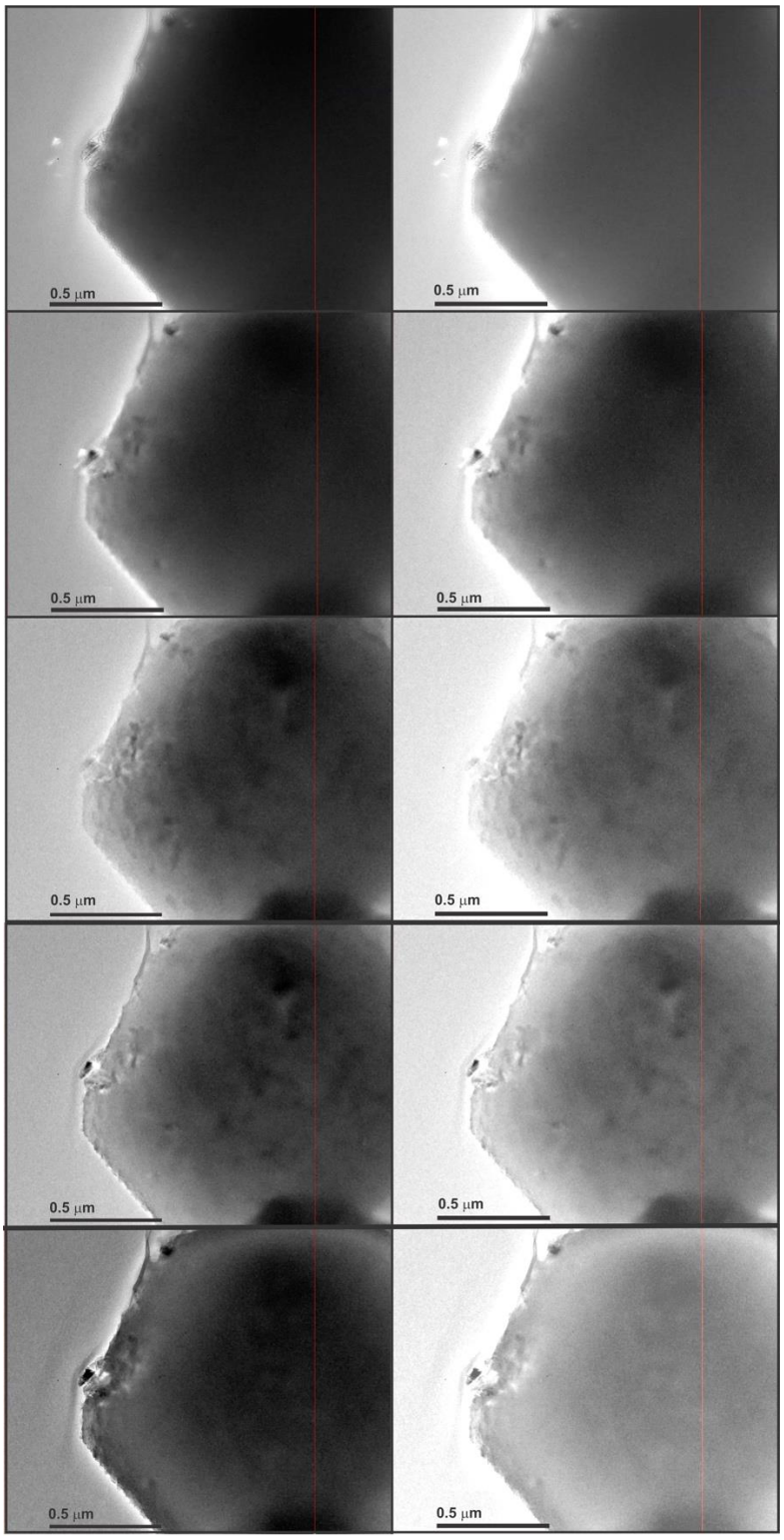

Figure S4. TEM images from video S1 in which the focus is gradually increased. Original images are in the left column, while images in the right have the brightness enhanced for clarity. The images indicate that nanodiamonds are dispersed within the ZIF-8 as opposed to being on the surface.

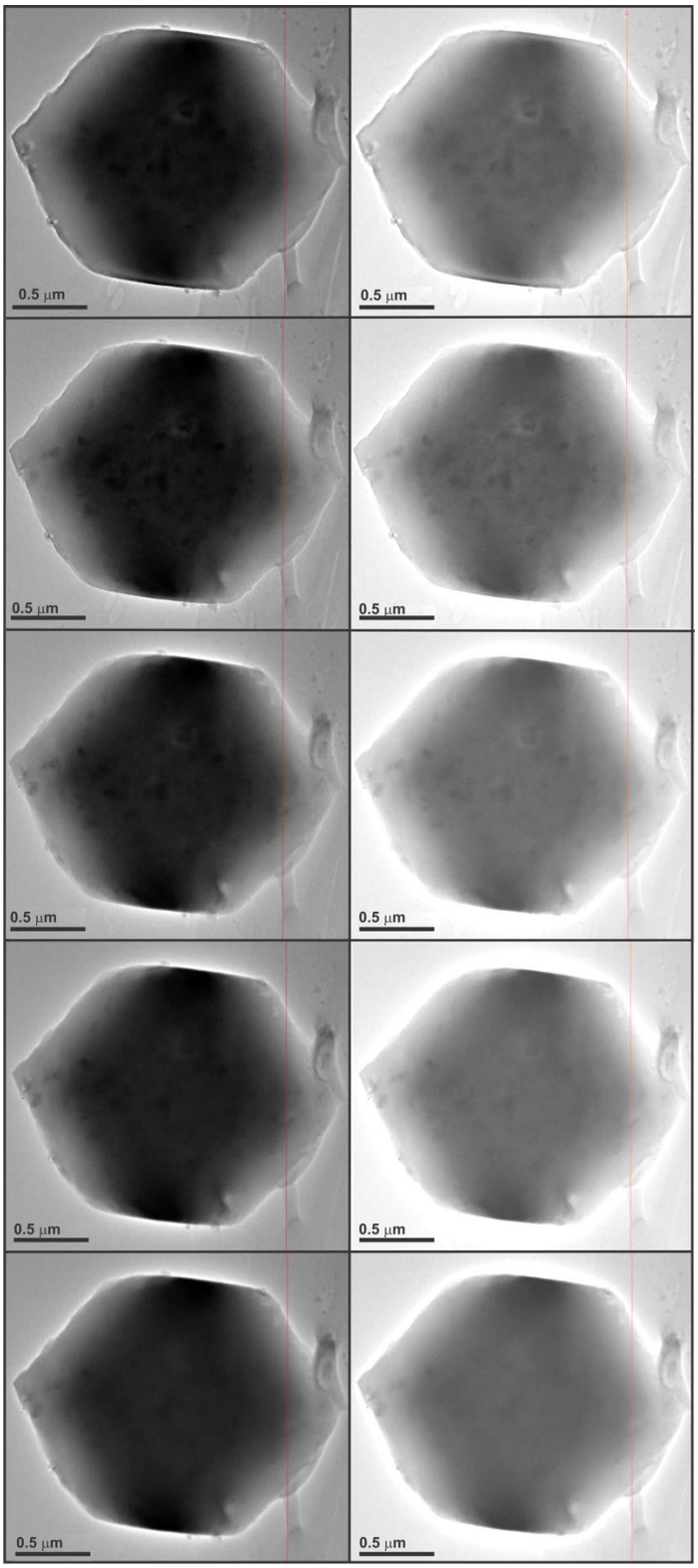

Figure S5. TEM images from video S2 in which the focus is gradually increased. Original images are in the left coluzmn, while images in the right have the brightness enhanced for clarity. The images indicate that nanodiamonds are dispersed within the ZIF-8 as opposed to being on the surface.

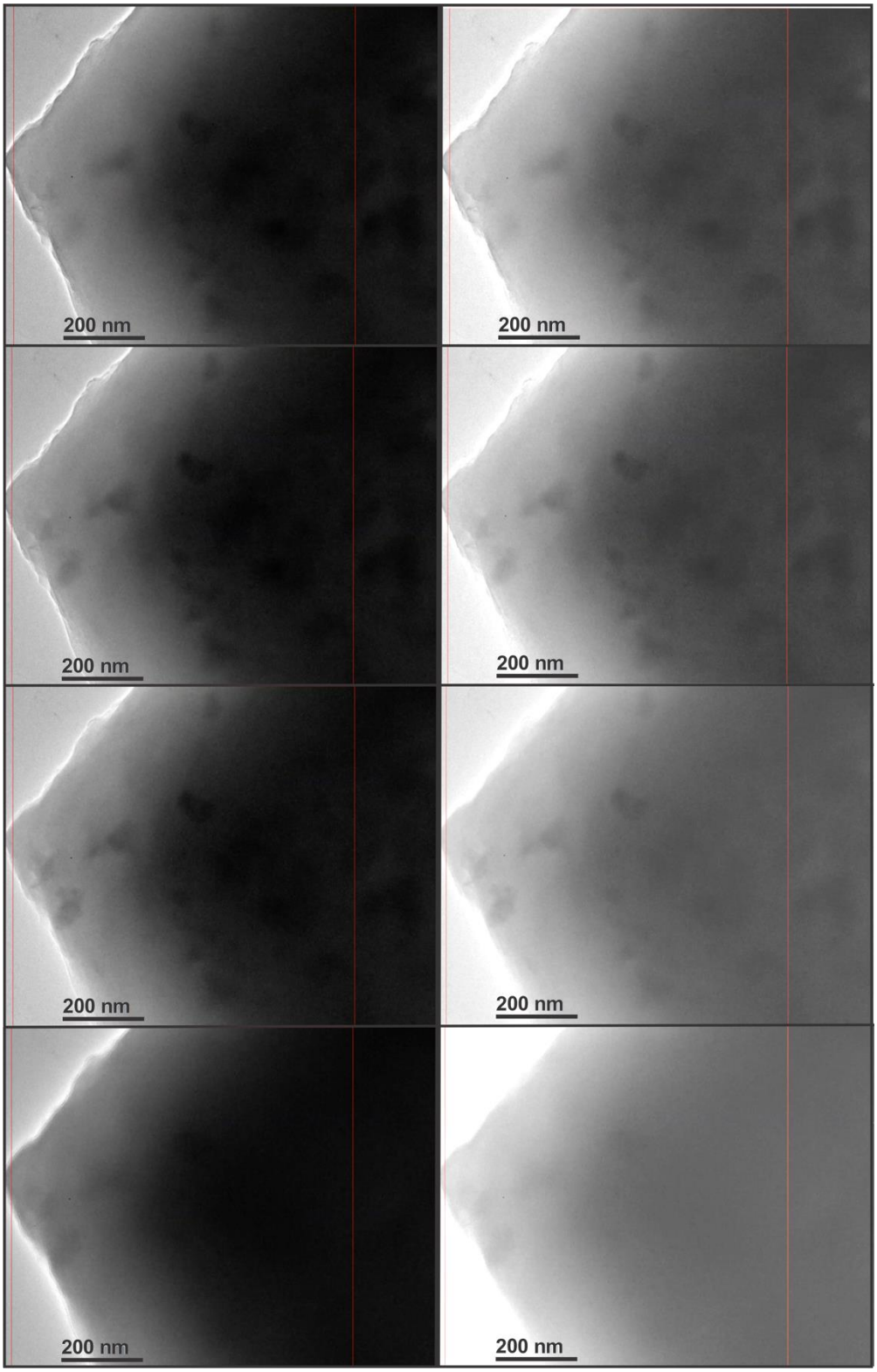

Figure S6. TEM images from video S3 in which the focus is gradually increased**.** Original images are in the left column, while images in the right have the brightness enhanced for clarity. The images indicate that nanodiamonds are dispersed within the ZIF-8 as opposed to being on the surface.

Table S1. Summary of XPS-Determined Binding Energies, and D-parameters

	Binding Energy (eV)			N/Zn Atomic	D-parameter
	C 1s	N 1s	Zn $2p_{3/2}$		
Nanodiamond	284.7	398.2	-	-	12.5
ZIF-8	285.0	399.0	1021.9	1.07	13.8
NDs@ZIF-8	285.0	398.8	1021.7	1.05	13.2

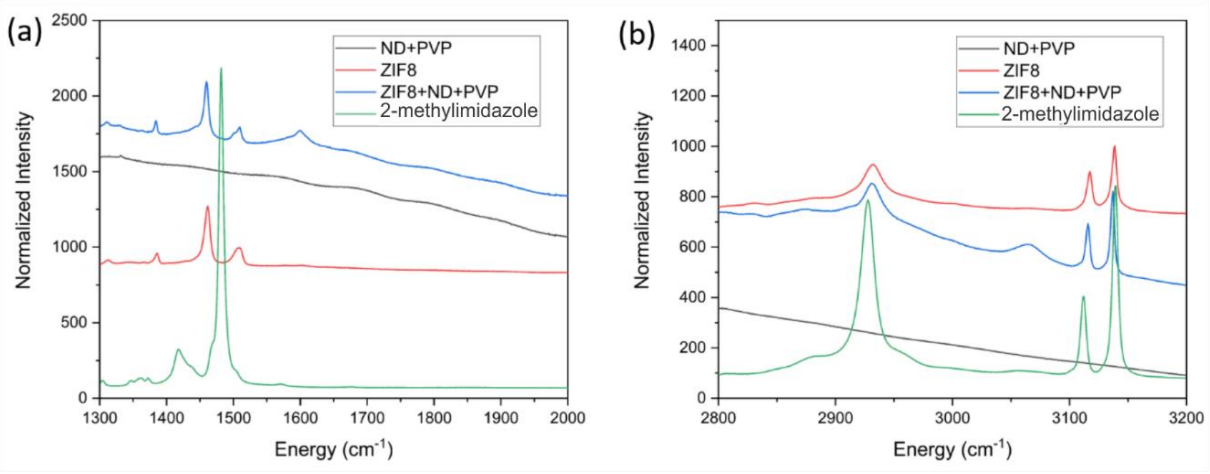

Figure S7. Raman spectroscopy comparative data of the PVP-capped nanodiamonds, pure ZIF-8, ZIF-8 encapsulated PVP-coated nanodiamonds, and 2-methylimzidazole**.**

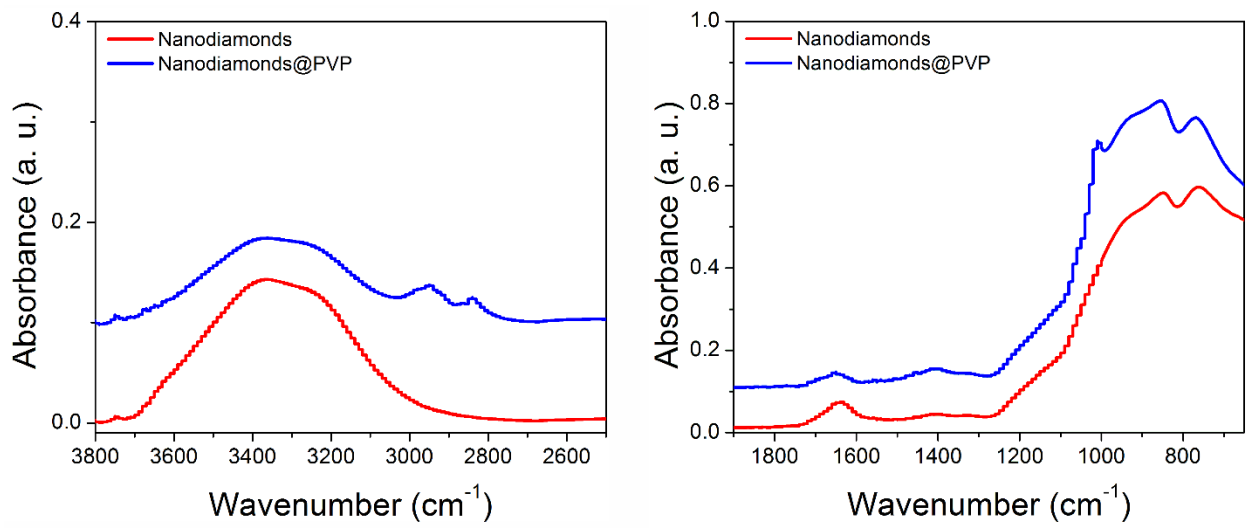

Figure S8. FTIR spectra of nanodiamonds (red) and PVP-capped nanodiamonds (blue). The nanodiamonds were in water and the PVP-capped nanodiamonds were in a water-methanol mixture. A dampening of the carboxylic acid OH stretch at 3400 cm^{-1} indicates hydrogen bonding between PVP and the nanodiamonds, and additional characteristic PVP peaks are observed at ~2943 cm^{-1}, ~2838 cm^{-1} ~1680 cm^{-1}, and ~1004 cm^{-1}.[1-2]

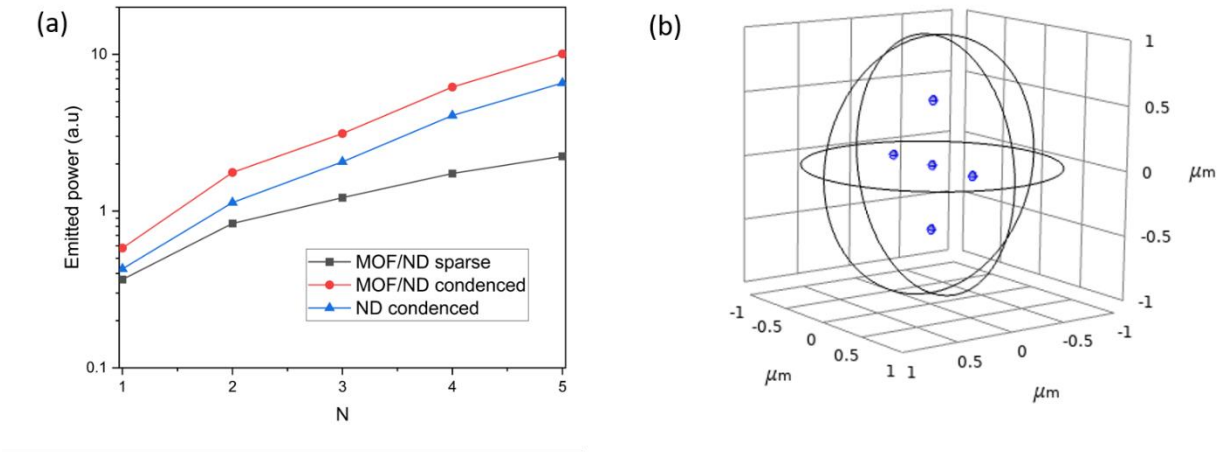

Figure S9. Modelling of nanodiamond spontaneous emission. Scaling of emission with increasing number of nanodiamond emitters. Each diamond sphere contained a single dipole emitter (a). Geometry of decoupled separated emitters in the ZIF-8 sphere (b)

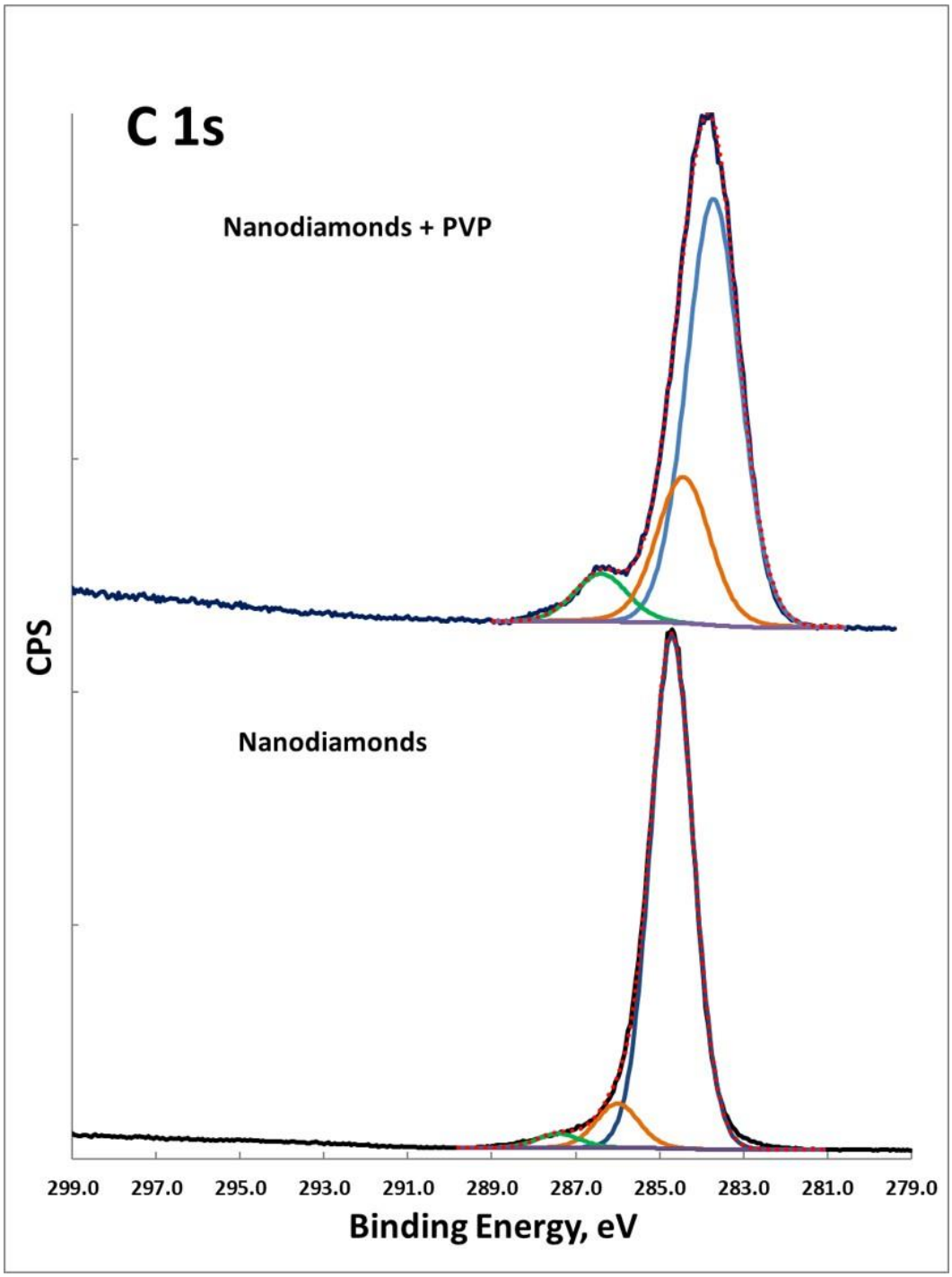

Figure S10. Comparative C 1s XPS spectra for nanodiamonds and nanodiamonds+PVP with binding energies referenced to the Fermi edge. The main C-C peak in nanodiamonds has a binding energy of 284.7 eV. Less intense peaks are located at 286.0 eV (C-O surface contamination and C-N) and 287.4 eV (C=O surface contamination). Similar peaks for Nanodiamonds + PVP are shifted by ~-1.0 eV, but higher binding energy peaks are now due to C-N and C=O from the PVP structure. Spectra were acquired under enhanced resolution with an analyzer pass energy of 13 eV and a step size of 0.05 eV

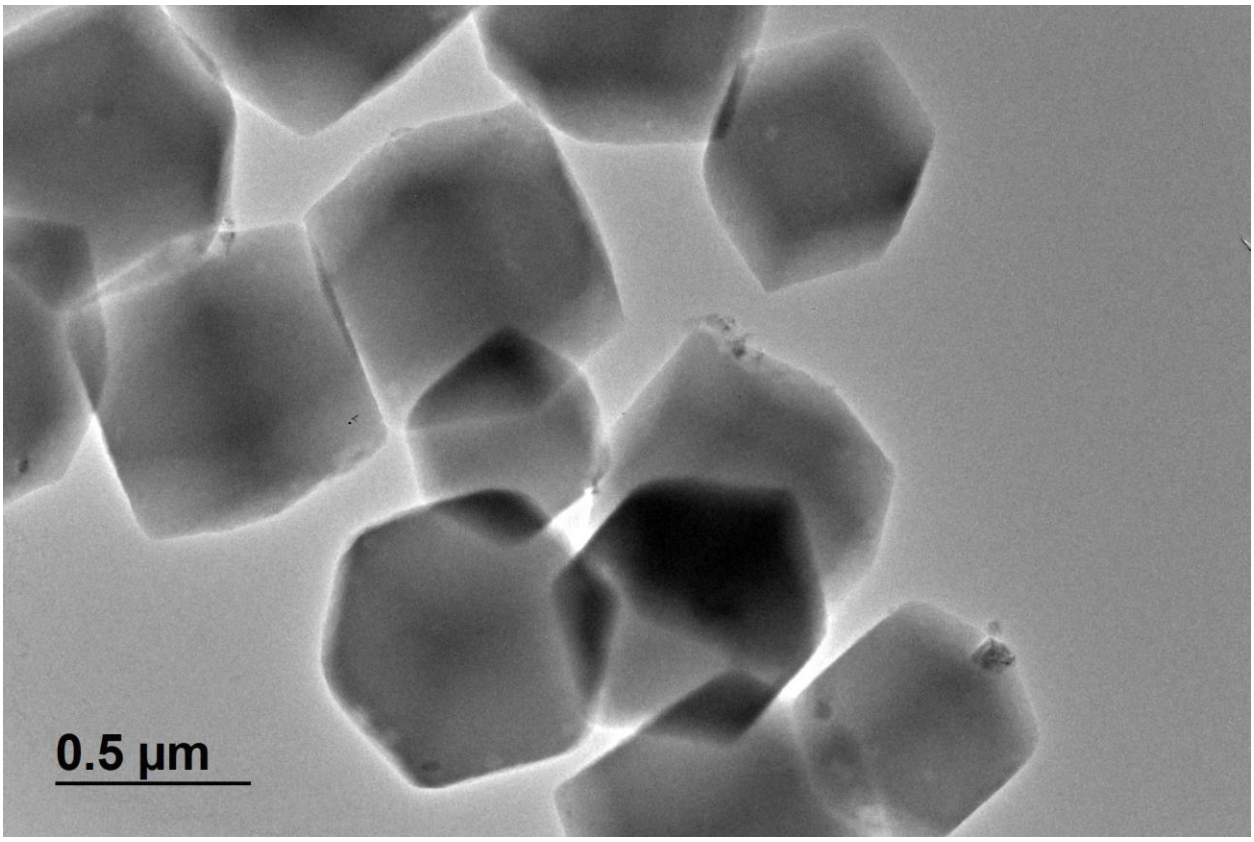

Figure S11. Wideout TEM image of ND@ZIF-8 composites synthesized using 7.5 µL of PVP-capped NDs.

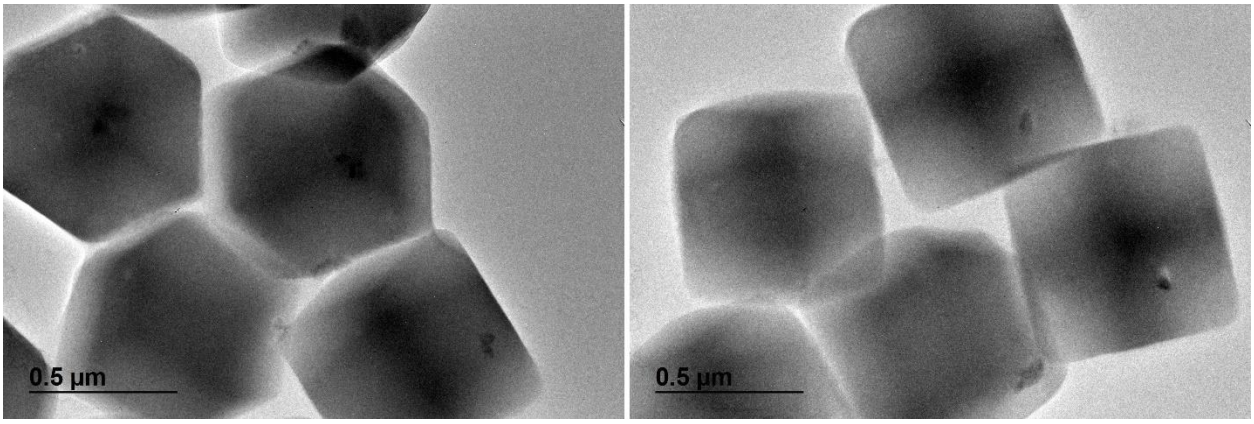

Figure S12. TEM images of ND@ZIF composites synthesized using 7.5 µL of PVP-capped NDs at higher magnification. Spots of higher contrast indicate the presence of a single ND within many of the MOFs.

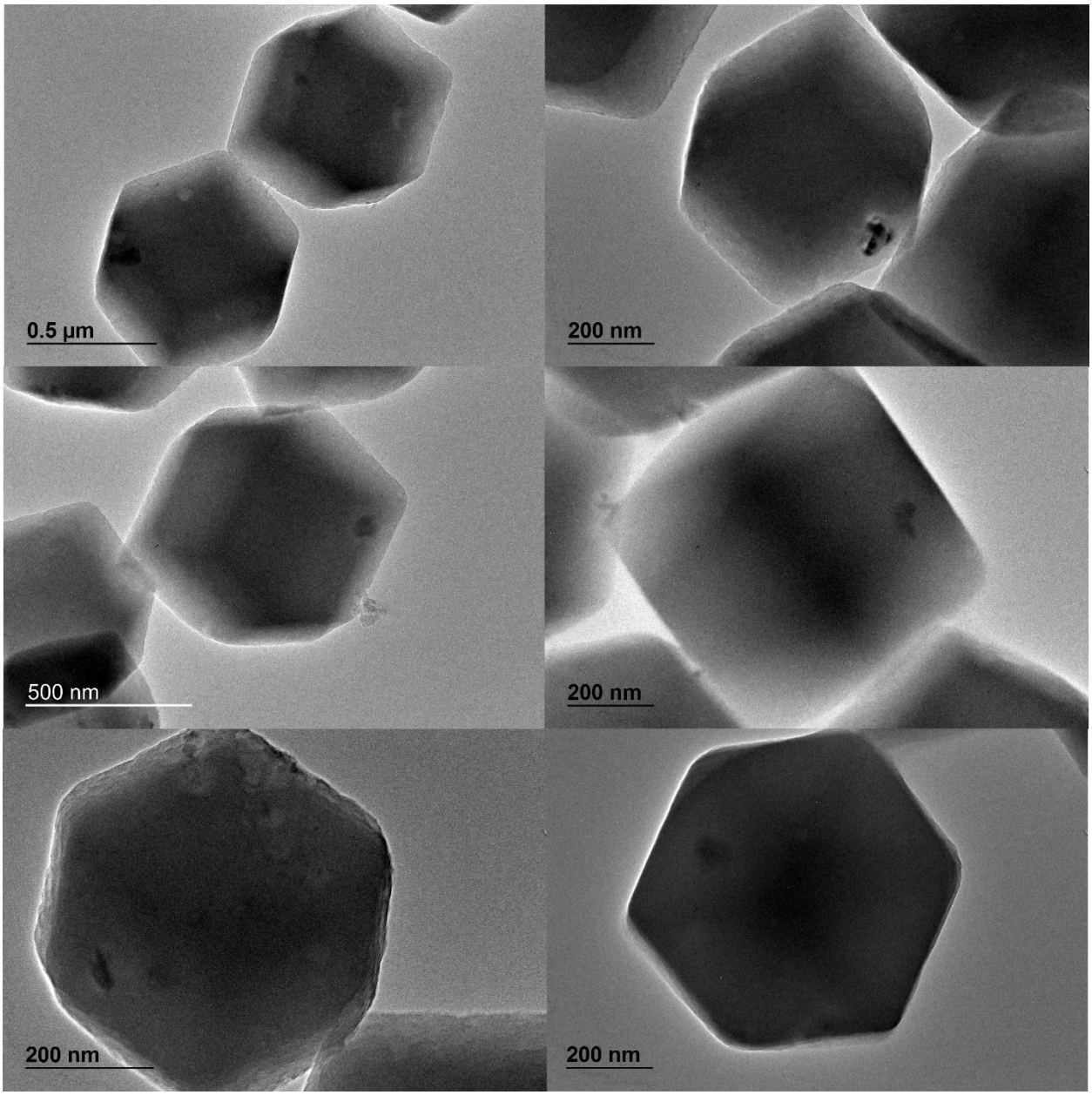

Figure S13. High magnification images of individual ND@ZIF-8 composites using 7.5 µL of PVP-capped NDs containing 1 ND per MOF.

References

1. Jung, H.-S.; Cho, K.-J.; Ryu, S.-J.; Takagi, Y.; Roche, P. A.; Neuman, K. C. Biocompatible Fluorescent Nanodiamonds as Multifunctional Optical Probes for Latent Fingerprint Detection *ACS Appl. Mater. Interfaces* **2020**, *12*, 6641-6650.

2. Attia, N.; Rao, J.; Geckeler, K. Nanodiamond–Polymer Nanoparticle Composites and Their Thin Films *J. Nanoparticle Res.* **2014**, *16*, 1-12.